Neurocomputing 551 (2023) 126510

Contents lists available at ScienceDirect

Neurocomputing

journal homepage: www.elsevier.com/locate/neucom

DeepInfusion: A dynamic infusion based-neuro-symbolic AI model for segmentation of intracranial aneurysms

Iram Abdullah [a], Ali Javed [a], Khalid Mahmood Malik [b,*], Ghaus Malik [c]

[a] Department of Software Engineering, University of Engineering & Technology, Taxila 47040, Punjab, Pakistan
[b] Department of Computer Science & Engineering, Oakland University, Rochester 48309, MI, USA
[c] Department of Neurosurgery, Henry Ford Hospital, Detroit 48202, MI, USA

ARTICLE INFO

Article history:
Received 3 March 2023
Revised 5 June 2023
Accepted 23 June 2023
Available online 28 June 2023

Keyword:
Neuro-symbolic
Diagnostic tool
Intracranial aneurysm
Deep Learning
Model infusion

ABSTRACT

The detection and segmentation of cerebral aneurysms is a crucial step in the development of a clinical decision support system for estimating aneurysm rupture risk. However, accurately identifying and segmenting regions of interest in two-dimensional (2D) medical images is often challenging, particularly when using deep learning (DL) methods on small datasets with limited annotated data. The accuracy of DL approaches is often affected by the availability of large, annotated training datasets that are required for effective deep learning. Additionally, when using DL to differentiate aneurysms from arterial loops in 2D DSA images, DL can fail to detect aneurysms in areas where dye concentration is low. To address these issues and enhance the reliability and accuracy of aneurysm detection and segmentation methods, incorporating medical expert-advised, hand-crafted features can provide a clinical perspective to DL methods. This approach can help to improve the performance of DL methods by providing additional information that is not captured in the data. To this end, a novel Neuro-symbolic AI-based DeepInfusion model is proposed which allows for the infusion of human intellect through hand-crafted features into deep neural networks (DNNs), thus combining the strengths of DL with the knowledge and expertise of medical professionals. The proposed approach includes a novel technique for dynamic layer selection and feature weight adjustment during the model infusion process. The performance of the DeepInfusion model is evaluated on an in-house prepared dataset of 409 DSA images, and experimental results demonstrate the effectiveness of the proposed method for the segmentation of cerebral aneurysms. The model achieves an IOU score of 96.76% and an F1-score of 94.15% on unseen DSA images. The model is also tested on two publicly available datasets of Kvasir-SEG polyp and DRIVE for vessel segmentation of retinal images. The results show a significant improvement compared to existing methods, which indicates the generalizability of the approach in medical segmentation. The complete code for DeepInfusion is available on our GitHub repository at https://github.com/smileslab/deep-infusion/blob/main/deepinfusion.ipynb.

© 2023 Elsevier B.V. All rights reserved.

1. Introduction

A cerebral, or intracranial, aneurysm is the focal dilation of an artery of the brain, resulting from a weakening of the interior muscular layer in the arterial wall. Accurate detection and segmentation of aneurysms are crucial in making informed decisions regarding clinical management [1]. Both invasive and non-invasive imaging methods [2,3] are used for diagnosing and managing cerebral aneurysms. Non-invasive methods, such as magnetic resonance angiography (MRA) and computed tomography angiography (CTA), are routinely used for diagnosing intracranial aneurysms. However, several case studies have reported discrepancies in aneurysm location and size using these methods [4]. Digital subtraction angiography (DSA), despite being an invasive technology, remains the gold standard for aneurysm detection due to its high sensitivity and specificity.

To develop a reliable decision support system for predicting subarachnoid hemorrhage, it is crucial to automatically detect and precisely segment intracranial aneurysms. However, this task is challenging due to various factors, including variations in aneurysm size, complex vascular anatomy, variations in image resolution, non-uniform dye concentration injected into aneurysms and different parts of arteries (see Fig. 1-a), as well as lighting and

* Corresponding author.
E-mail address: mahmood@oakland.edu (K.M. Malik).

https://doi.org/10.1016/j.neucom.2023.126510
0925-2312/© 2023 Elsevier B.V. All rights reserved.

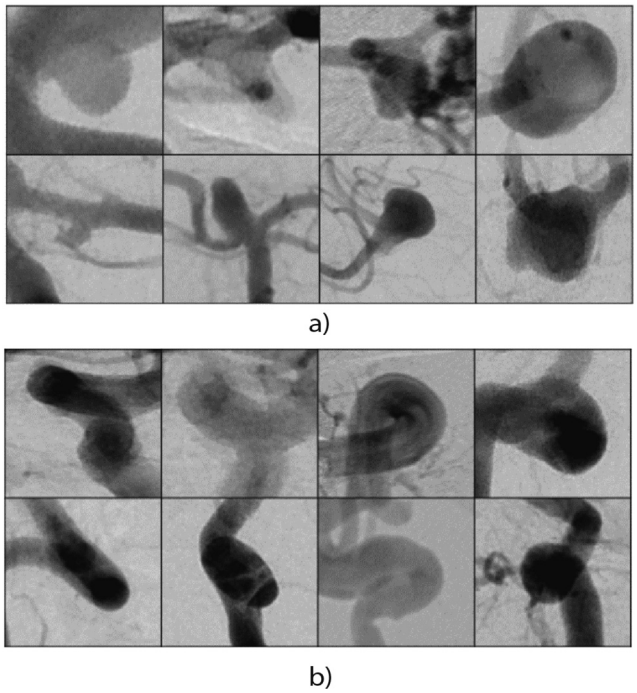

Fig. 1. a) Morphological and geometrical diversity of cerebral aneurysms in 2D DSA images. b) Morphological and geometrical diversity of vascular loops in 2D DSA images.

intensity variations in samples resulting from the diversity of imaging equipment used. The presence of noise and other artifacts further complicates the accurate segmentation of detected aneurysms. Detection becomes even more challenging when vascular loops are present in the DSA image (see Fig. 1-b) because their geometrical structure and localized dye concentration may closely resemble that of an aneurysm. Additionally, various morphological and geometrical features must be considered for rupture prediction, such as irregularities in the aneurysm wall, daughter domes, vertebral dominance, perpendicular height and width, neck diameter, aspect and size ratio, height-to-width ratio, the angle relative to the vessel, and diameters of adjacent parent and daughter-vessels [5,6]. Unfortunately, the current less accurate detection and segmentation techniques act as bottlenecks in accurately determining these features. There is a significant research gap primarily because of the limited availability of DSA images.

Medical imaging studies have addressed the issue of detecting and segmenting regions of interest (ROIs) using either conventional machine learning (ML) or deep learning (DL) methods across various medical image modalities. ML algorithms can learn diagnostic patterns highlighted by medical professionals, but their accuracy in aneurysm segmentation using hand-crafted features may be impacted by data bias and model design. In contrast, DL techniques have proven successful in overcoming these challenges, but their black-box nature, the requirement of large training datasets, and the inability to incorporate human feedback during training may make them less attractive for clinical use. It is crucial to establish the relevance of DL models in clinical analysis by designing reliable diagnostic systems that incorporate domain expert knowledge. However, DL models for medical imaging face additional challenges due to limited imaging data acquired in nonstandard settings with varied equipment and heterogeneous, imbalanced sample data. Additionally, labeled data may be sparse, noisy, or entirely missing. Incorporating domain expert knowledge into DNNs can help overcome these challenges, but current methods that concatenate handcrafted and deep features or infuse them into the last layer lack flexibility in dealing with the diversity of medical imaging data. In rare diseases like cerebral aneurysms, building datasets on the scale required for DL approaches is challenging due to regulatory mechanisms that prevent privacy infringements. Without sufficient data, DL models cannot learn all the patterns needed to achieve the desired outcomes.

Deep learning methods may be inadequate in detecting aneurysms in DSA images under certain circumstances, even in the presence of extensive data sets that are currently unavailable. For example, if the region of interest has a low dye concentration, the DL models may fail to detect the aneurysm due to the limited availability of similar samples in the training dataset. In such situations, the expertise of medical professionals in identifying aneurysms based on characteristics such as shape, edges, and borders can be integrated with DL models to improve the accuracy of detection and segmentation. However, the challenge lies in determining how to incorporate these clinical practices into DL models. As such, there is a need to explore strategies for integrating medical expertise into DL models to achieve improved outcomes in aneurysm detection and segmentation in DSA images. This study aims to develop a neuro-symbolic AI approach that incorporates domain professionals' expertise into a DL model for detecting and segmenting cerebral aneurysms from DSA images. To the best of our knowledge, no existing methods have dynamically integrated clinical knowledge into DL models for medical image analysis. Domain knowledge can be incorporated into DL models through clinical knowledge in the form of a knowledge graph [7], diagnostic patterns for rule-based learning [8], and feature knowledge recommended by domain experts. This study aims to integrate hand-crafted features based on domain knowledge into a DL neural network. It addresses several research questions, such as effectively incorporating domain knowledge into DL models, the impact of incorporating domain knowledge on DL model performance, and effective methods for combining domain knowledge with DL models to improve medical image analysis. The study will examine research questions related to selecting optimal layer depth, the weighting of domain knowledge and deep features, and criteria for selecting appropriate infusion level and weight factors to achieve optimal outcomes in medical image analysis. The major contributions of the proposed research work are: (see Fig. 2).

- This study examines the feasibility and methodology of integrating domain knowledge in the form of hand-crafted features into a DNN for medical image analysis.

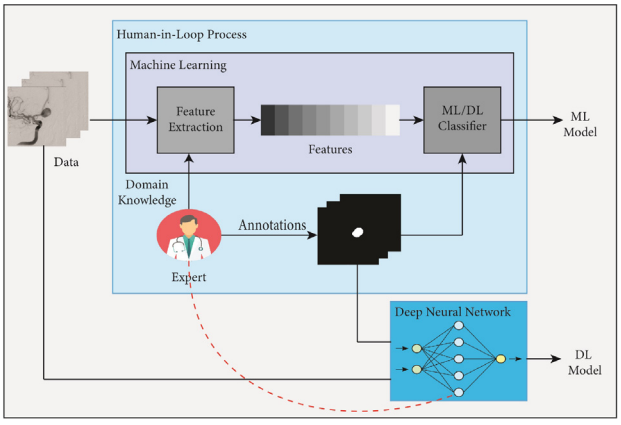

Fig. 2. Conceptual view of expert's knowledge infusion in the Deep Neural Networks.

- This paper introduces a novel DeepInfusion model that leverages domain expertise to enhance cerebral aneurysm detection and segmentation by identifying the optimal layer within the deep neural network. Additionally, a dynamic mechanism to adjust the weight proportion of DNN model and knowledge models is developed. The resultant output of the machine learning model developed on the knowledge of domain experts is infused as attention in the Deep segmentation network layer. Since DNN itself also processes the same image input, the induced attention of the knowledge model assists the DNN in significantly improving its performance.
- Theoretical explanation and rigorous experimentation on knowledge infusion and its effect on accurate segmentation from a highly diversified angiogram dataset are presented.

The paper is organized as follows: Section II presents a discussion of existing literature, while Section III describes the proposed method. Section IV briefly introduces the dataset used for experimentation, highlights the challenges presented by diverse angiograms, and presents experimental results. Further discussions are provided in Section V, and Section VI concludes the paper with future directions.

2. Related work

Computer-aided diagnostics (CAD) approaches can assist neurosurgeons in aneurysm detection and segmentation. Existing CAD techniques for aneurysm detection primarily rely on DSA imaging modality, which is widely regarded as the gold standard in this field. However, limited attention has been given to the segmentation of aneurysms in DSA images. Previous research has examined both learning-based and non-learning-based automation techniques to achieve the objective of aneurysm detection.

Existing non-learning studies have employed different enhancement or shape-oriented filters to address the aneurysm detection problem. For example, Arimura et al. [9,10] designed a 3D selective enhancement kernel for intracranial aneurysms detection with high sensitivity and low false positives (FPs). However, these methods [9,10] have limited application utility for unknown scenarios as they considered only a few aneurysms to derive the rules used for eliminating FPs. Similarly, different shape-oriented filters, based on the eigenvalues of the hessian matrix, were proposed in [11,12] for aneurysm detection. Jerman et al. [12] proposed a blob enhancement filtration method based on the eigenvalues of the multiscale 3D Hessian. This method is independent of the intensity and size of blobs, making it suitable for detecting small blob-like structures such as aneurysms. Additionally, a volume rendering method based on extending the maximum intensity difference accumulation (MIDA) [13] was developed to enhance the visualization of regions containing the aneurysm. Performance of this method [12] was evaluated on just 30 DSA and 10 CTA images. Arimura et al. [9] proposed a method based on a shape-based difference imaging approach for aneurysm detection. Multiple thresholding was employed on grayscale images followed by skeletonization to determine the initial candidates. The region-growing technique was applied to identify the candidate regions. A similar effort of detecting the aneurysm using morphological analysis was proposed in [14].

Learning-based methods are commonly employed to achieve better classification performance, however, this comes at the expense of increased computational cost as compared to non-learning methods. The current learning-based methods have employed both traditional machine learning and deep learning methods for aneurysm detection. Existing methods have used different traditional machine learning classifiers such as KNN and SVM. For example, Zafar et al. [15] proposed a feature vector of the shape and texture of aneurysm areas and used them to train a KNN classifier for aneurysm detection. Hanaoka et al. [16] proposed a feature set based on histograms of triangular paths in the graph (HoTPiG) to detect cerebral aneurysms. Region growing technique was used to extract the arterial region. An undirected graph was used to create a feature descriptor HoTPiG for each voxel of the foreground region. Finally, HoTPiG features were used to train the SVM to label each voxel as an aneurysm or healthy region. In [17], an automated rule-based scheme was used in combination with statistical features and quadratic discriminant analysis to detect the aneurysm. Yang et al. [18] proposed an automated method for detecting intracranial aneurysms. This method involved extracting geometrical features from points of interest (POIs) and applying empirically determined rules to select the most probable POIs for aneurysms. In [19], an automated technique was introduced for detecting cerebral aneurysms. Specifically, the blob-ness filter was applied to identify potential candidates of the aneurysm. K-means clustering was used to compute volumes of interest in the filtered image. A rule-based scheme was then applied in combination with thresholding to detect the aneurysms. Similarly, in [20], a semi-automated technique based on Geodesic Active Contours was proposed for aneurysm segmentation. However, this method has limitations when dealing with overlapping features in vasculature loops and aneurysms. The advancement of neural networks, particularly deep learning (DL), in recent decades has motivated researchers to explore its utility in various domains for improved performance compared to conventional machine learning (ML) algorithms. Some research studies [21,22] have applied convolutional neural networks (CNNs) to detect aneurysms in different image modalities. Jerman et al. [21] proposed a learning-based framework that utilized intra-vasculature distance mapping and CNNs for aneurysm detection in 3D cerebral angiograms. The arterial structure in the angiogram image was enhanced using a Hessian filter. Intra-vascular distance maps were then computed to the edges of vascular structures, and CNNs were trained and validated using these DSA images for aneurysm detection. However, this approach only utilized a very limited dataset of 15 DSA images, which may not be sufficient for effective application of deep learning techniques. Similarly, in [22], a deep neural network combined with a maximum intensity projection algorithm was employed for aneurysm detection. The deep network consisted of two convolutional layers, two max-pooling layers, and two fully connected layers. In experiments conducted by Liao et al. [23] and Zeng et al. [24], high-dimensional sequences of DSA frames were used. Zeng et al. [24] trained a slightly modified conventional VGG model for detecting aneurysms, using 133 frames for each sample. However, processing such a large amount of data incurs a computationally expensive overhead. Tao [25] believed that 3D-DSA (three-dimensional digital subtraction angiography) leads to more accurate detection and reduces misclassification rates. The method employed Bayesian optimization and thresholding to draw conclusions for automatic detection.

Although segmentation of aneurysms is crucial for estimating the risk of rupture, very few studies [26,27] have prioritized segmentation as the primary task. Among these, Liu et al. [26] proposed the 3D-Dense-UNet model for segmenting detected aneurysms in 3D-DSA images. The segmentation performance of the model was evaluated with a correlation coefficient of 0.77, which demonstrated a discrepancy of 1 mm and 2.5 mm compared to expert measurements of the segmented aneurysms. Jin et al. [27] proposed a DL-based framework to assist neurologists in evaluating and contouring intracranial aneurysms from 2D DSA sequences during diagnosis. The network incorporated both spatial and temporal information and achieved an accuracy of 89.3% for

aneurysm detection. In terms of segmentation, the dice coefficient (DC) score was used and obtained a DC of 0.533. However, both of these studies are computationally expensive due to the use of either 3D images or selected sequences of 2D images. Moreover, the segmentation of aneurysms is not as accurate as required for precise estimation of the risk of rupture.

Segmentation is a significantly challenging task in medical imaging due to the complex and demanding nature of medical datasets. In a comprehensive study conducted by Bizopoulos et al. [28], the researchers investigated the impact of various cutting-edge deep learning models on different performance metrics using medical imaging. Specifically, they extensively investigated the results of lung segmentation using popular DL models such as Pyramid Scene Parsing Network (PSPnet), Linknet, and Unet providing a detailed comparison. The study [28] explored the performance of these models for lung segmentation. By inspecting the obtained results, it was found that the Unet model demonstrated remarkable performance, confirming its practicality and effectiveness in the field of medical image segmentation [29]. PSPnet [30] focuses on capturing global context through its pooling module, which is valuable for addressing scaling variations and identifying abnormalities in structural components, it tends to overlook local features that hold importance in medical detection. On the other hand, Linknet [31] introduces skip connections that facilitate the flow of feature information between the encoder and decoder, resulting in improved segmentation. However, Linknet is unable to accurately identify boundaries, leading to missed details in the segmented areas. In contrast, Unet [29] combines the advantages of both local and global feature extraction. It achieves this by incorporating an encoder-decoder structure with skip connections that maintain a strong link between the encoder and decoder. This architecture allows Unet to leverage the benefits of capturing global context while preserving crucial local features. By preserving information from the encoder layers and enabling the flow of details through skip connections, Unet excels in capturing fine details and accurate boundaries in segmented areas.

Recognizing the significance of making sensitive decisions, the inclusion of domain knowledge becomes a crucial element in attaining the desired level of accuracy. Integrating domain knowledge with the DL model can be a valuable approach to enhance the effectiveness of segmentation. In their work, Yu et al. [32] presented a multimodal transformer (MT) model for generating image captions. The core idea of their proposed method is to utilize multiple detectors and feed their output to the network. MT performs sophisticated reasoning across multiple models and produces descriptive captions. The paper discussed the process of merging multiple detector features at the beginning of the network, but it did not explore the interaction at the depth of the network. In [33], Zhang et al. demonstrated the efficacy of computing residual vectors using diverse centroids and subsequently combining them by assigning distinct weights to each residue vector before their aggregation. According to their findings, these weights contribute to enhancing the diversity of the residue sum, thereby boosting the discriminative capabilities of image features. These studies [32,33] emphasize the importance of network-level interactions, similar to our network. However, the limitations of their works arise from the failure to incorporate variations in the input at the network level. These variations can be introduced based on the feedback provided by domain experts. Our study is motivated by the need to address this limitation by incorporating diverse knowledge-based inputs at the network level. The objective is to enhance the performance of segmentation process.

3. Proposed method

This section explains the proposed methodology for infusing domain expert knowledge into deep learning models. It also elaborates on the importance of pre-processing in complex medical angiograms. In addition, knowledge exploitation on different layers of a deep neural network is discussed in detail.

3.1. Pre-processing

The pre-processing step is designed based on prior knowledge about aneurysm detection by medical experts. Physicians consider three essential DSA features for aneurysm detection: 1) circular or elliptical shapes in the DSA, 2) consistency of blood, represented as dark areas in the region of interest, and 3) the artery with which the aneurysm is associated. These three distinct pieces of information can be passed on to three other channels of the image. As DSA images are monochromatic, the red, green, and blue channels in the image do not significantly vary or contribute to detection.

1) Shape-based feature extraction

The nature of an aneurysm emphasizes the significance of circular regions in DSA, which can improve detection accuracy. Shape-based points of interest (POIs) are computed from DSA images by combining connected pixels in each binary DSA to form groups and computing the center of each group or shape. These shapes are classified based on properties such as circularity, convexity, and inertia ratio to extract the POIs. While the shape of a saccular aneurysm is circular, it is not a complete circle, and the minimum circularity value of 0.1 is used to extract shapes with circular tendencies, accounting for the imperfect circles of aneurysms. Convexity helps to identify closed shapes with some hollow areas, referred to as the convex hull. The minimum convexity value of 0.1 is used to locate hollow circular shapes, accounting for the inconsistent blood flow in aneurysms.

2) Color quantization for blood consistency

Assessing the consistency of blood in DSA images can be challenging due to the different shades of color used to depict its appearance. To make consistency checking more effective, color quantization can be used to reduce the number of color shades in the image. The K-Mean clustering method was employed for achieving quantization, and Fig. 3 shows the outcome of this process.

3) Vasculature extraction

The extraction of the vascular structure from DSA images is crucial for precise aneurysm detection and segmentation. To achieve this, the dimensions of the original image are reduced by transforming the color image into grayscale. Due to the invasive nature of DSA images, the intensity values are limited to a small range. To enhance the distribution of intensities, contrast enhancement techniques such as histogram equalization are applied. However, the contrast-enhanced image often contains a significant amount of noise that needs to be reduced for the precise extraction of the arterial structure. To address this, a median smoothing filter of size 5×5 is applied to reduce the noise. Additionally, in order to extract the vessel area with high precision, the image is converted into a two-level binary image. The information preserved in the original pixels of the angiogram has its own importance. With consideration for the effect of the original intensity, the two-level

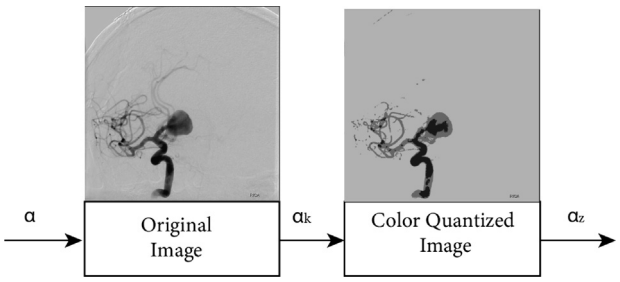

Fig. 3. Color Quantization for Blood Consistency Checking.

binary image is further processed to exclusively retain the original pixels representing the vascular architecture. The details of the vascular extraction process are presented in Fig. 4.

4) Expert guided input preparation

Instead of using the original DSA image as input for the DL model, we adopted a three-stage approach that incorporated expert-guided pre-processing. This information was encoded into three channels of an RGB image. The first channel contained shape-based points of interest, while the second and third channels contained information on blood consistency and vasculature architecture, respectively. The expert-guided input was subsequently processed using the ResNet101 backbone.

3.2. Knowledge extraction using hand-crafted features

In the field of medical image analysis, incorporating domain knowledge is critical for developing robust automated diagnostic tools. To gain a comprehensive understanding of aneurysm detection, we consulted an experienced domain expert. By leveraging their expertise, we accurately labeled aneurysms. Specifically, we extracted patches of images that contained aneurysms and stored them as representative samples of the aneurysm class.

1) Points of interest extraction

In the context of aneurysm detection, medical practitioners initially focus on identifying circular or elliptical shapes within blood vessels. Our investigation shows the significance of shape-based features, as advised by experts, in DSA images. Nevertheless, in-depth experimentation revealed that neither shape-based features nor deep features in isolation (as outlined in Section 3) are adequate for precise aneurysm detection, since vascular loops share analogous anatomical characteristics. Consequently, the shape-based image resulting from the pre-processing stage serves as input for the knowledge extractor, wherein each shape is cropped and stored as a point of interest (POI). Thus, POI could be both the vascular loops and aneurysms.

Algorithm 1: Knowledge Extraction

Require: α_x ▷For α_x Fig. 5.
Require: T ▷Minimum threshold for infusion level.
Ensure: $POI[] = findcountour(\alpha_x)$
  $i \leftarrow length(POI)$
  while $i \neq 0$ **do**
    $C \leftarrow predict(POI[i])$
    if $C \leqslant T$ **then**
      $remove - POI[i] - from - \alpha_x$
    end if
    $i - -$
end while

2) Region of interest (ROI) extraction

The region of interest in the DSA image is the aneurysm. Vascular structures with circular or elliptical shapes can resemble aneurysms, highlighting the need for POIs to distinguish them from actual aneurysms. A balanced dataset of aneurysms and vascular loops, each containing 174 samples, was prepared from the training images. A binary CNN classifier was developed using these samples to distinguish between aneurysms and loops. Based on the classifier's output, patches containing loops were removed (Algorithm 1), and the remaining patches were treated as ROIs. Each ROI contained visual information and a confidence level (C), indicating the classifier's probability of categorizing the shape as an aneurysm. The study created images of high- and low-probability aneurysms based on the confidence level (Fig. 5). The difference (d) between the two categories could be calculated using Eq. 1.

$$d = \frac{S(N) \times (1 - T)}{N} \tag{1}$$

N is the total number of layers in the deep learning model. T is the minimum acceptable confidence level, which is acceptable to categorize the POI as an aneurysm.

$$S(N) = \frac{N}{t} \tag{2}$$

Because of the complexity, not every layer can be selected as an infusion level. Therefore, $S(N)$ is introduced to add a shift (Eq. 2) between the infusion levels. The shift can be calculated by dividing N by the total number of allowed infusion levels (t).

3.3. Knowledge infusion in DNN

U-Net [34] is a widely used convolutional neural network architecture that has shown remarkable performance in medical image

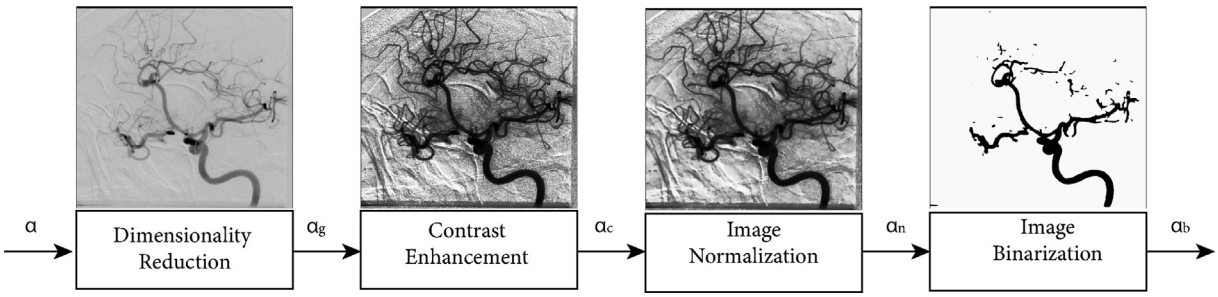

Fig. 4. Depiction of step-by-step process of vasculature extraction from 2-D DSA images.

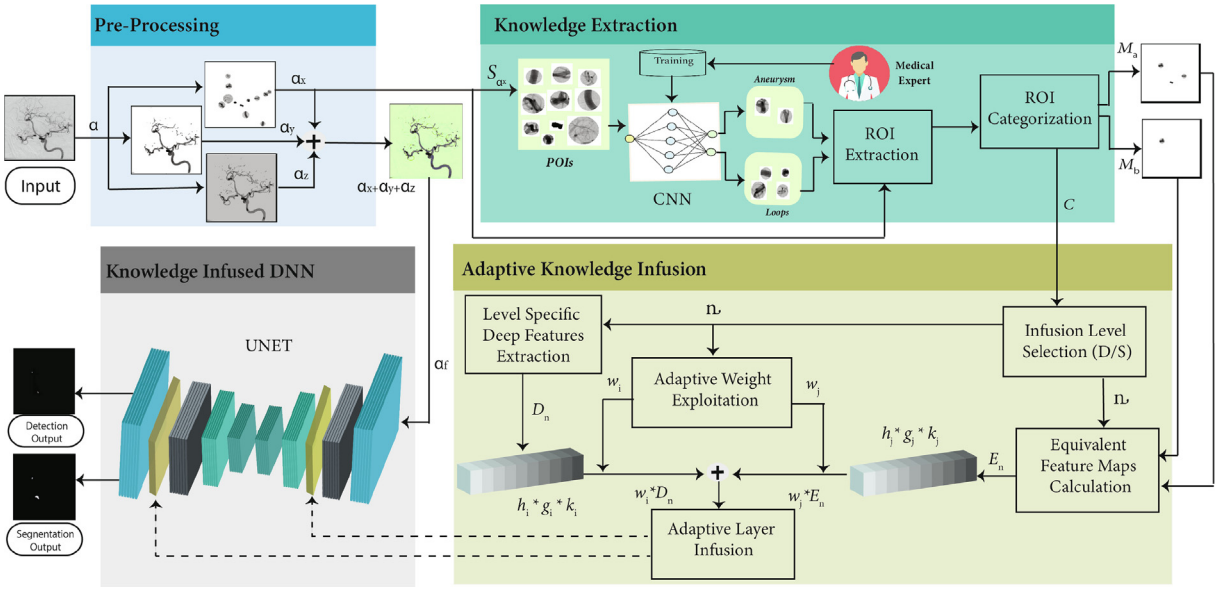

Fig. 5. Framework for Intracranial Aneurysm Detection and Segmentation.

classification tasks, particularly in segmenting and identifying organs and abnormalities. However, despite its widespread adoption, several challenges remain, including the scarcity of annotated data, which reduces the performance and robustness of the model, particularly for rare diseases such as cerebral aneurysms. To address this issue, incorporating expert-designed hand-crafted features, such as geometric and anatomical features, into deep learning layers can improve the model's performance [35]. While these features are typically added at the input layer or fused at the classification level using ensemble learning, there is no previous work that dynamically exploits the "attention" introduced by domain experts. To address this gap, we propose a method that directly applies hand-crafted features to the layers of U-Net, rather than relying on black-box feature extraction or skip connections that depend solely on the loss functions. This section describes the proposed approach for leveraging deep neural network knowledge and discusses the details of early or late infusion, along with weight adjustments.

1) Infusion Level/Layer Selection

In the proposed method, the first and the most important parameter is the selection of infusion level/layer (l) in the U-Net Network. The infusion level decides the interaction of the deep neural network with the expert-guided knowledge. The knowledge extracted in the previous step corresponds to the confidence level of the classifier used in knowledge extraction. Our hypothesis is that if the confidence of the knowledge/handcrafted-based classifier is low, the U-Net should exploit the feature maps of the ROI extracted by the classifier early on. Conversely, if the classification confidence is very high, the U-Net should exploit this information at the deeper layers.

$$l = \frac{(C - T)}{d} \tag{3}$$

The confidence level (C) of ROI with the minimum acceptable confidence level (T) is an important factor in infusion level decisions. In the proposed method, the infusion level is calculated by dividing the difference between C and T with the difference (d) between each category (Eq. 3).

$$n = l \times S(N) \tag{4}$$

In Eq. 4, n represents the layer number at which the infusion takes place.

2) Deep feature extraction

The encoder-decoder-based deep neural network [34] plays an important role in medical image analysis. The proposed deep learning model is built using the ResNet101 block to maintain the identity function and improve the accuracy of the detection. The encoder is a traditional convolutional network that comprises the recurring application of two 3×3 convolutions followed by a rectified linear unit (ReLU). For the down-sampling, a 2×2 max pooling operation with stride 2 is used. The number of features doubles at each down-sampling step. Decoding is followed by up-sampling where 2×2 convolution is applied on the feature map. The up-sampling cuts down the features channels by half. Also, each layer in the decoder is concatenated with the respective cropped feature map from the encoder layer. At the last layer, the feature vector of 64 components is converted to the number of classes by performing the 1×1 convolution. Each layer of encoder and decoder is also stacked with Resnet101 layers to learn the complex features in the angiograms. Keeping in view the availability of limited data, the encoder is designed to use the ImageNet weights. The rest of the layers are designed to use skip connections with the encoder to utilize the pre-weights and learn about the specific domain dataset. The network is further enhanced by infusing the knowledge at different levels. For this purpose, the infusion level-based deep features (Eq. 5) are extracted from the deep learning model.

$$D_n = h_i \times g_i \times k_i \tag{5}$$

The number of filters is represented by k_i while the h_i and g_i are dimensions of the image.

3) Equivalent feature maps calculation

The knowledge cannot be exploited directly to the deep learning layers because of the abstract nature of deep features and different dimensions of tensors (Eq. 5). Based on the level of infusion, the equivalent feature map needs to be calculated. For this purpose, we introduced a dynamic sub-network generation mecha-

nism to calculate the maps according to the level of infusion. Each knowledge category input is processed from the infusion level-based sub-network and calculates the equivalent feature map (Eq. 6).

$$E_n = h_j \times g_j \times k_j \tag{6}$$

Here the number of filters are represented by k_j while the h_j and g_j are dimensions of the image. E_n is equivalent to D_n.

Algorithm 2: Adaptive Multi-Level Infusion

Require: α_x, α ▷For $\alpha_x and \alpha$ Fig. 5.
Ensure: $POI[] \leftarrow S_{\alpha_x}$ ▷S Extract POIs from Image.
  $ROI_a[] = empty$
  $ROI_b[] = empty$
  $z \leftarrow length(POI), i \leftarrow 0$
  while $i < z$ **do**
    $C \leftarrow predict(POI[i])$
    if $C \geqslant 0.75$ **then**
      $ROI_a \doteq POI[i]$
    end if
    if $C \geqslant 0.50 \& C < 0.75$ **then**
      $ROI_b \doteq POI[i]$
    end if
    $i++$
  end while
  $M_1 \leftarrow ROI_a$ ▷M Merge ROIs to Image Fig. 5.
  $M_2 \leftarrow ROI_b$
  $N \leftarrow length(DL_{model})$
  $t \leftarrow N$ ▷Total number of allowed infusion levels.
  $T \leftarrow min(C)$ ▷Minimum acceptable confidence level.
  $d \leftarrow (1-T)/N$
  $m \leftarrow 0$
  $w \leftarrow 1$
  $w_0 = w/t + 2$
  $k \leftarrow 1$
  while $m \leqslant t$ **do**
    $j \leftarrow 0$
    $C_m = (m \times d) + T$
    $n \leftarrow (C_m - T)/d$
    $w_i = (n+1) * w_0$
    $w_j = w - w_i$
    while $j \leqslant n$ **do**
      $D_j \leftarrow featuremap(\alpha)$
      if $n == j$ **then**
        $E_j \leftarrow featuremap(M_k)$
        $k++$
        $D_n = w_i * D_j \otimes w_j * E_j$
      else if $n \leqslant j$ **then**
        $E_j \leftarrow featuremap(M_k)$
      end if
      $j++$
    end while
    $m++$
  end while

4) Adaptive weight exploitation

The weights of external and deep feature maps are an important aspect of infused U-Net. The proposed adaptive knowledge exploitation method considers the position of the layer and calculates the dynamic weights. The depth of the network is calculated using the infusion level. Based on the calculated depth, the weight distribution is selected. The weight distributions show the weights assigned to knowledge features and deep features. We analyzed different weights of knowledge w_i to deep features w_j in our experiments. The results show that for early infusion the w_i must be relatively greater than w_j and vice versa for late infusion. The equal distribution of weights is effective in the middle of the network. The maximum weight w assigned to deep or knowledge features can be *1*. The initial weight w_0 value needs to be calculated as a starting point.

$$w_0 = \frac{w}{t+2} \tag{7}$$

w_0 is calculated by dividing the w by t with the shift of *2*. The factor *2* is introduced to avoid the assignment of maximum (*1*) or minimum (*0*) value to each feature.

$$w_i = (l+1) \times w_0 \tag{8}$$

The weight of the knowledge-based feature (w_i) is calculated from infusion level selected for the said features and initial weight. The remaining weightage is assigned to deep features (w_j).

$$w_j = w - w_i \tag{9}$$

5) Adaptive layer infusion

The deep features specific to each level (denoted as D_n) are merged with the corresponding knowledge-based feature map (E_n). The weighting of the deep features and knowledge-based features is determined based on the infusion level (l), following the dynamic weight calculation process as discussed in the criteria.

$$L_{n+1} = (w_i \times (h_i \times g_i \times k_i)) \otimes (wj \times (h_j \times g_j \times k_j)) \tag{10}$$

The prepared knowledge-infused layer is added at the selected infusion level and the rest of the network remains the same. The output of the infused layer goes to the next layer of the network. The infusion not only increases the number of layers by one but also another input carrying knowledge is added that represents the guideline for the deep network layer. The adaptive layer infusion operates in two ways. Firstly, the choice of layer depends on the task objective. For example, for the detection of all aneurysms, infusion mostly works better in either the initial or final layers, whereas for segmentation, the middle layers are more appropriate. Secondly, instead of categorizing tasks into two distinct groups, we categorize the confidence into confidence intervals, and the infusion is determined dynamically based on the criteria outlined in Algorithm 2. To validate the hypothesis of dynamic infusion, initially only two intervals and threshold were chosen. However, in dynamic infusion, the weights and layers are dynamically calculated. Algorithm 2 explains the overall mechanism of adaptive infusion based on two intervals. Within Algorithm 2, the *predict*() function represents the mechanism of prediction of the CNN classifier that takes POI and returns the C where the C above 50% is considered as potential ROI. Each ROI is associated with a confidence level that greatly influences the decision-making process for adaptive infusion level selection. The algorithm utilizes two fixed parameters for early and late infusion, which are determined based on the C of the ROI. For late infusion, the ROI with a C of 75% is utilized, while the early infusion of the ROI occurs within the C of $50\% - 75\%$.

4. Experimental results

In this section, we provide a comprehensive account of various experiments conducted to assess the detection and segmentation performance of DeepInfusion. Additionally, we also include the specifics of the dataset used in these experiments. Our investiga-

tion focused on two key factors: firstly, the efficacy of the model in incorporating knowledge into different layers of deep learning; secondly, the influence of layer selection and weight assignment on the deep and knowledge-based features.

4.1. Dataset selection

Choosing an appropriate dataset for detecting and segmenting aneurysms presents several challenges, such as varying equipment, angiogram techniques, high-intensity imaging, limited image availability, and the location and appearance of cerebral aneurysms. Furthermore, due to medical ethics, patient datasets cannot be publicly accessed for research, so angiograms must first be anonymized before analysis. Additionally, expert knowledge is necessary to identify intracranial aneurysms from the arterial structures. To assess our proposed method, we employed 409 2D digital subtraction angiography images. In clinical settings, 2D images are typically used for diagnosis, whereas we generated 3D images specifically for experimentation purposes. To target the 2D images, we collected single-frame angiograms from a time series imaging study based on six views: medial and lateral, proximal and distal, and superior and inferior. The dataset consists of images that depict the occurrence of aneurysms in nine different arteries, namely ACOM, Basilar, ICA, MCA, PCA, PCOM, PICA, supraclinoid, and SICA. Out of the dataset's images, 15 do not have aneurysms, while the rest contain one or more aneurysms, with a total of 436 aneurysms marked by an expert. Among these aneurysms, 339 are saccular, and the remaining 31 are fusiform, included to test segmentation's robustness. Previously, existing approaches only focused on saccular aneurysms. The average aneurysm area is 2550 pixels, ranging from a minimum of 145 pixels to a maximum of 22880 pixels. Loop presence in the angiogram is another important factor that complicates the aneurysm detection process. The average loop area in angiograms is 2024 pixels, ranging from a minimum of 99 pixels to a maximum of 15916 pixels. The collected 2D DSA angiograms are partitioned into training and testing datasets in a 4:1 ratio. These angiograms are labeled by a neurosurgeon for segmentation.

4.2. Evaluation parameters

The proposed system is evaluated in two phases. The first phase involves evaluating the accuracy, precision, and recall of the knowledge extractor. In the second phase, the aneurysm detection results are evaluated using the F1-Score, while the aneurysm segmentation is evaluated using intersection over union (IOU), in knowledge infused DNNs.

4.3. Experimentation

This section provides different experiments to investigate the importance of adaptive knowledge infusion on different layers of the model. Moreover, we also examined the importance of defining the preferences of knowledge in deep learning features and the effect on aneurysm detection.

a) Knowledge extraction

The objective of this experiment was to evaluate the reliability of knowledge extraction by developing a model that could distinguish between aneurysms and loops. To accomplish this, we extracted 349 aneurysms and an equal number of diverse loops from a training set of 319 angiograms, ensuring class balance. We then trained various traditional machine learning algorithms, such as Logistic Regression, Linear Discriminant Analysis, K-Nearest Neighbors, Classification and Regression Trees, Random Forest, Naive Bayes, and Support Vector Machine, but the accuracy of the results was low, as shown in Fig. 6. Consequently, we decided to use a convolutional neural network as a backend classifier, with handcrafted features that integrated domain knowledge. The knowledge extractor is tested on 127 equal number of aneurysms and loop slices for classification. Overall, the accuracy of the classifier is 90%, and the precision, and recall is 86% and 95% respectively. The confusion matrix in Fig. 7 shows the performance of the classification on test data.

b) Effect of knowledge infusion at different layers in deep neural network

The knowledge extracted in the previous experiment can be a guiding factor for the deep layers in the model. For this purpose, an additional experiment is conducted to observe the effect of knowledge infusion on different layers of deep learning model. Selection of the layer in DNN is a critical factor considering the confidence of knowledge classifier. Our first goal is to find out the effect of infusion at different layers. The idea behind the selection is to observe the behavior of the deep learning model by infusing the knowledge at three different positions i.e. start, end, and middle. The other challenge of this investigation is to infuse high-level knowledge with deep features. The deep features abstraction depends on the position of the layer. To deal with this challenge, the knowledge embeddings are generated to make the high-level knowledge equivalent to deep features by introducing the abstraction. The five different models are designed and evalu-

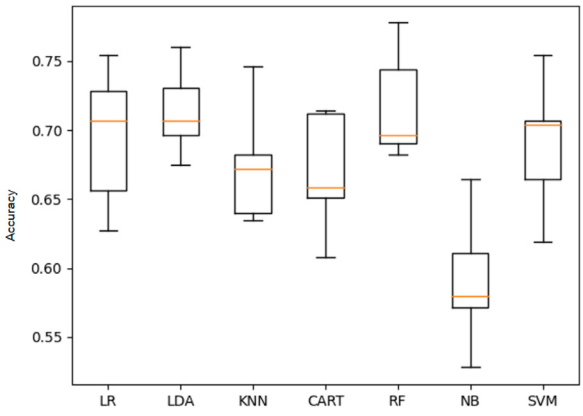

Fig. 6. Performance comparison of ML classifiers for knowledge extraction.

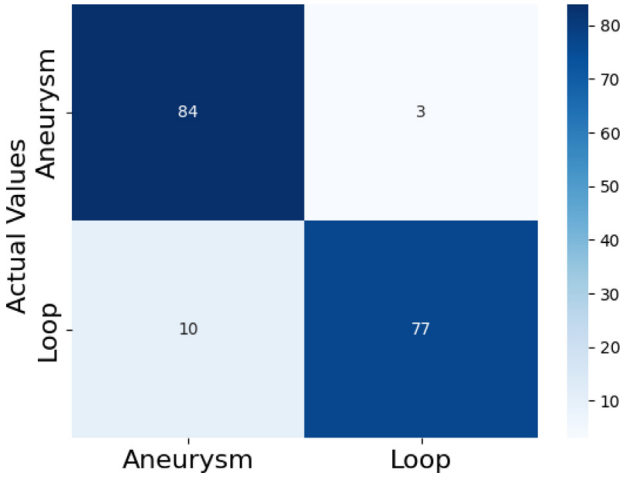

Fig. 7. Confusion Matrix for Knowledge Extractor.

Table 1
Results on different knowledge infused layers.

		Knowledge Infused Layers				
Parameter	**UNET**	**380**	**278**	**209**	**106**	**57**
Training						
Loss	0.0005	0.0013	**0.0003**	0.0018	0.0021	0.0016
IOU	0.8498	0.9170	0.9418	0.9411	**0.9450**	0.9107
Accuracy	0.9997	0.9993	**0.9998**	0.9990	0.9989	0.9991
F1-Score	0.8309	**0.8684**	0.7800	0.8201	0.8105	0.8614
Validation						
Loss	0.0004	0.0010	**0.0003**	0.0012	0.0015	0.0013
IOU	0.8778	0.9124	**0.9661**	0.9576	0.9413	0.9052
Accuracy	0.9998	0.9994	**0.9998**	0.9994	0.9993	0.9993
F1-Score	0.8323	0.8634	0.7900	0.8014	0.7447	**0.8555**
Testing						
Loss	**0.0004**	0.0012	0.0003	0.0022	0.0016	0.0015
IOU	0.7930	0.7646	0.8518	0.8586	**0.9030**	0.7638
Accuracy	0.9998	0.9993	**0.9998**	0.9988	0.9991	0.9992
F1-Score	0.6357	0.8553	0.6052	0.6724	0.6980	**0.8554**

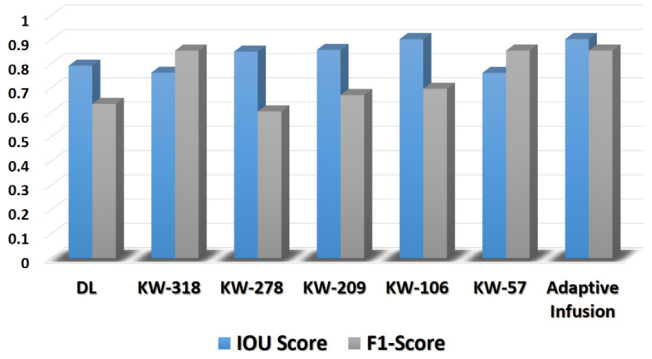

Fig. 8. Comparison of Performance Measure with respect to Infusion Level.

ated quantitatively for different evaluation parameters on test data. The results of knowledge infusion at layer 380, 278, 209, 106 and 57 are presented in Table 1. The results of model infusion are compared with the deep learning model. The positive impact of Knowledge (KW) infusion on various layers of deep learning models is apparent. Fig. 8 compares the performance of each layer using selected measures, and the variations in these measures demonstrate the impact of KW infusion. Most layers experience an increase in IOU score following infusion, indicating improved accuracy in mask extraction. However, the layer that contributes to better segmentation may differ from the one that contributes to better detection. For instance, while layer 106 is the best for segmentation, layer 57 is the most suitable for detection among the various infusion levels.

In Fig. 8, the performance of models infused at various layers is compared. Infusions at layers 106 and 209 appear to accurately segment the aneurysm, closely matching the ground truth. Conversely, infusions at later layers such as 278 and 380 detect small shape-based features as potential aneurysms. Additionally, the early infusion is more effective at detecting aneurysms with low brightness. The results suggest that both early and late infusions improve detection, while middle layers are more suitable for segmentation. If the knowledge extractor is unable to differentiate between the aneurysm and vasculature loop then the model accepts it as a potential aneurysm. But the middle layers like 106 and 209 re-consider the features along with deep features and filter those areas, which are misclassified by the knowledge extractor. The low intensity or small sized aneurysms, which are usually missed by the DL model can be detected via early infusion. By decreasing the threshold of the IOU-Score to 0.2 an improvement in segmentation can be observed (Table 2).

c) Optimizing the weights of DNN and KW features in infusion

In the previous experiment, the infusion assigned equal weights to both knowledge-based features and deep features. The present experiment seeks to investigate the impact of weight distribution on infusion. Layers 106 and 209 demonstrated positive outcomes in the segmentation task during the prior experiment. To examine the significance of weight distribution, layer 106 was selected for infusion, and the experiment was conducted using different weight ratios of DNN and knowledge features, specifically 60:40, 50:50, 40:60, and 30:70. The weight ratios in this experiment are represented by the first and second terms of the ratio, indicating the weights assigned to the deep features and knowledge features, respectively. Table 3 demonstrates the impact of weight distribution, revealing that while weights have no effect on accuracy, they do influence IOU and F1-Score. Table 3 also emphasizes the importance of selecting an appropriate layer and weight distribution for optimal outcomes. Increasing the weights assigned to knowledge features from 50 to 60 leads to an increase in the IOU score for the training data, although no variation is observed in the test data

Table 2
Effect of IOU-Score Threshold on Segmentation.

Threshold	**UNET**	Knowledge Infused Layers				
		380	**278**	**209**	**106**	**57**
0.5	0.7930	0.7646	0.8518	0.8586	0.9030	0.7638
0.3	0.8664	0.8485	0.8990	0.9109	0.9342	0.8475
0.2	0.9158	0.9065	0.9273	0.9468	**0.9597**	0.9043
0.1	0.8708	0.8945	0.8937	0.9018	0.9201	0.8624

according to the qualitative analysis in Fig. 9. In contrast, decreasing the weight to 40 for knowledge-based features causes a change in the IOU score in both the training and test data. Further decreasing the weight to 30 results in significant improvement in both the train and test data, suggesting that a 30:70 ratio is close to optimal for layer 106. Overall, this experiment highlights the importance of weight distribution in infusion and demonstrates that the appropriate selection of layer and weight distribution can lead to improved results.

d) Adaptive infusion in DNN

The previous two experiments have demonstrated that the effectiveness of infusion is dependent on the infusion level/layer and the distribution of weights. However, an important question arises as to how to dynamically select the layer of the DNN model and weights for both knowledge and deep features. As discussed in the methodology, the proposed dynamic adaptive infusion levels depend upon the total number of allowed infusions. If the t is 2 then the thresholds will be 0.5 and 0.75. This means that low-confidence knowledge is infused at the beginning layers (e.g. level 57) and high-confidence knowledge is infused at the later layers (e.g. level 246) of the DNN. The results indicate that loss reduces when categorized external knowledge criteria are enforced. Additionally, there is significant improvement in F1-Score, although the segmentation performance is not optimal. Despite this, the performance of all parameters is improved. To further observe the effect, t is selected 3 leading to the calculation of new thresholds i.e. 0.5, 0.67, and 0.83. The introduction of these new threshold values enables three levels of infusion. The results (Table 4) reveal improvements in both the IOU-Score and F1-Score, underscoring the significance of adaptive infusion in enhancing both classification and segmentation. This approach overcomes the limitations of single-layer infusion, which typically improves either segmentation or classification alone. Therefore, dynamic infusion emerges as a preferable choice for enhancing overall detection and segmentation accuracy, fulfilling the needs of the medical field. Therefore, it is intuitive to use adaptive knowledge infusion, which involves dynamically selecting the infusion layer and weights based on

Table 3
Comparison of weighted infusion $w_j : w_i$ i.e. deep features: Knowledge features.

	Parameter	Weighted KW-Infusion on Layer 106			
		60:40	**50:50**	**40:60**	**30:70**
Training	**Loss**	0.0021	0.0021	0.0021	0.0021
	IOU	**0.9560**	0.9450	0.9540	0.9546
	Accuracy	0.9989	0.9989	0.9989	0.9989
	F1-Score	0.8070	**0.8105**	0.8059	0.8055
Validation	**Loss**	0.0015	0.0015	0.0015	0.0015
	IOU	0.9718	0.9413	0.9729	**0.9734**
	Accuracy	0.9993	0.9993	0.9993	0.9993
	F1-Score	**0.7385**	0.7447	0.7374	0.7366
Testing	**Loss**	0.0017	0.0016	0.0016	0.0016
	IOU	0.9597	0.9597	0.9591	**0.9602**
	Accuracy	0.9991	0.9991	0.9991	0.9991
	F1-Score	**0.6986**	0.6980	0.6966	0.6946

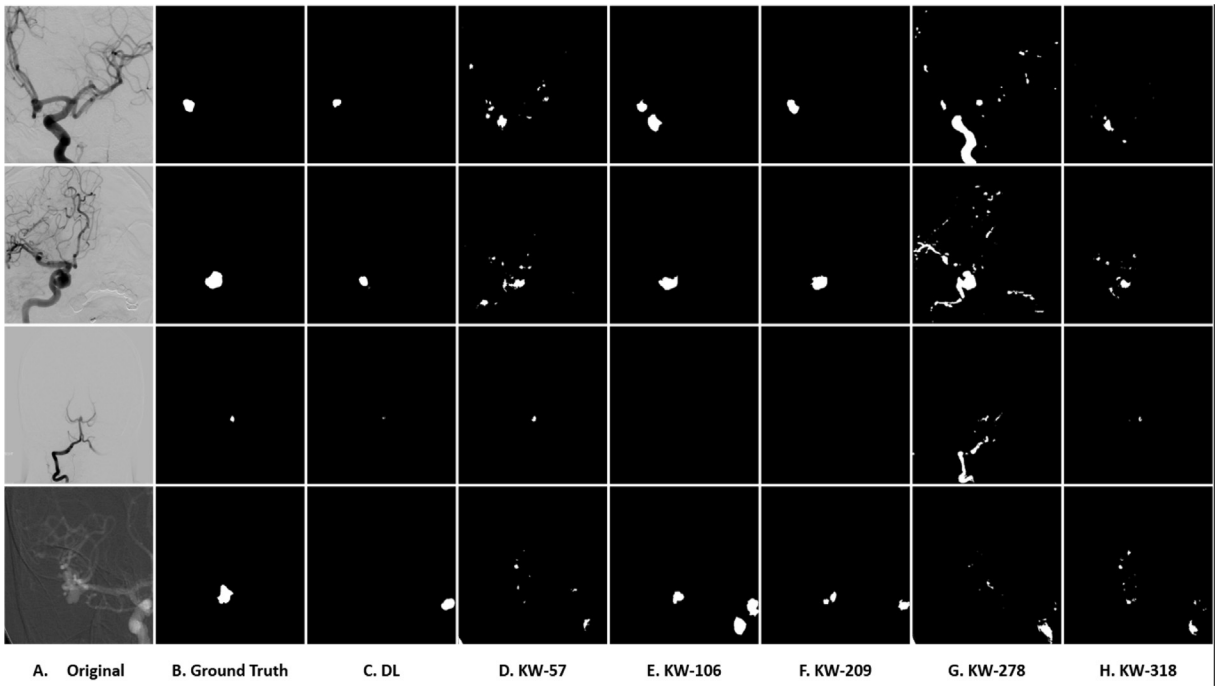

Fig. 9. Impact of knowledge exploitation on different deep learning layers.

the confidence level of the knowledge extractor/classifier. This approach allows for the infusion of external knowledge at appropriate layers of the DNN, which leads to improved results for all parameters. Ultimately, the use of adaptive knowledge provides a promising solution for achieving better performance in DNN-based tasks. Table 4 compares the performance of four different methods for image segmentation and detection. The first method is the UNET segmentation algorithm, static infusion at layer 106 for segmentation and layer 57 for detection. The third and fourth methods are two-level and three-level adaptive infusion. The results show that the three-level-adaptive infusion approach performs better than the other three methods regarding all parameters. It achieves the highest IOU score and F1-score. The F1-score for the adaptive infusion approach is particularly high, indicating a good balance between precision and recall. The results suggest that the adaptive infusion approach is a promising method for image segmentation and detection.

e) Ablation study

To assess the impact of the proposed system on reliable aneurysm segmentation, an ablation study was conducted. The study focused on evaluating the influence of key steps within the proposed method, namely hand-crafted feature extraction, knowledge infusion, weight exploitation, and adaptive infusion. The experimental results of segmentation in terms of IOU were analyzed to examine the individual contributions of each step in the knowledge infusion process to the network's overall performance. The results of this analysis can be observed in Table 5. By systematically studying and comparing the performance of the system with and without each step, valuable insights were gained regarding the effectiveness and significance of incorporating knowledge infusion techniques. It has been observed that the optimal layer for segmenting intracranial aneurysms is different from the optimal layer for the detection of these aneurysms. This explains why the experiment (Section 4-c. Optimizing the Weights of DNN and KW Features in Infusion) yielded superior results compared to the experiment (Section 4-d. Adaptive Infusion in DNN). The adaptive infusion was specifically devised to address both the detection and segmentation objectives for intracranial aneurysms. However, the possible reason for the relatively lower performance of adaptive infusion can be the selection of specific layers for infusion and the categorization of ROIs into only two categories of high and low confidence. To enhance adaptive infusion's effectiveness, it would be beneficial to expand the number of categories based on confidence levels and increase the infusion levels. By implementing these modifications, the adaptive infusion has the potential to exhibit significantly improved performance.

f) Comparative analysis of the proposed and contemporary models

We conducted an experiment to evaluate the performance of our model in comparison to our previous studies [5,15]. For the experiment, we utilized the same data collection procedure and a subset of our current dataset. The results are presented in Table 6, which shows a significant improvement in accuracy. These results demonstrate that a knowledge infusion is a promising approach for developing medical diagnostic systems, as it addresses the limitations of small datasets in deep learning models. To present the strength of the base network, we conducted a comprehensive evaluation by comparing it with state-of-the-art segmentation methods such as Linknet, PSPNet, and FCN. These well-established methods were specifically chosen to benchmark the performance of the base network on our dataset. Meanwhile the effect of introducing a knowledge module in segmentation models is observed across different networks. The IOU score of these methods was carefully analyzed and compared in Table 7. By conducting a comprehensive comparison, we were able to thoroughly analyze and evaluate the base network in comparison to other segmentation networks. This analysis enabled us to identify and emphasize the strengths and advantages of the base network over the alternative segmentation networks. Additionally, our comparison highlights the significance of knowledge infusion. The incorporation of additional information or features, through techniques like knowledge infusion, can enhance the performance and capabilities of segmentation networks.

Table 6
Comparison with Existing Approaches.

Method	No. of Images	Accuracy
ISADAQ [5]	59	86.00%
KNN [15]	209	95.00%
CNN + SIF [24]	300	98.98%
Proposed	409	**99.97**%

Table 4
Comparison of deep learning with different knowledge-infused networks.

Parameters	UNET	Segmentation (Layer = 106)	Detection (Layer = 57)	2-Level Adaptive Infusion	3-Level Adaptive Infusion
Loss	0.0004	0.0016	0.0015	0.0092	0.0102
IOU	0.9158	0.9602	0.9043	0.9354	**0.9676**
Accuracy	0.9998	0.9992	0.9991	0.9995	0.9997
F1-Score	0.6356	0.6946	0.8554	0.9323	**0.9415**

Table 5
Ablation Study.

Experiment	Hand-Crafted Features	Knowledge Infusion	Weight Exploitation	Adaptive Infusion	IOU Score
DNN	No	No	No	No	0.9158
Effect of Knowledge Infusion at Different Layers in Deep Neural Network	Yes	Yes	No	No	0.9597
Optimizing the Weights of DNN and KW Features in Infusion	Yes	Yes	Yes	No	0.9602
Adaptive Infusion in DNN	Yes	Yes	Yes	Yes	**0.9676**

Table 7
Comparison of Segmentation with state-of-the-art Techniques.

Segmentation Models	IOU-Score	
	DL	KW-DL
UNET	**0.9158**	**0.9354**
FCN	0.8748	0.8645
PSPNet	0.8696	0.8906
LinkNet	0.8778	0.9129

Table 8
Performance Comparison on Public Kvasir-SEG and DRIVE Test datasets.

	Kvasir-SEG		DRIVE	
	DL	KW-DL	DL	KW-DL
Loss	0.1344	0.1358	0.1224	0.1315
IOU	0.6015	0.6335	0.5784	0.5930
Accuracy	0.9462	0.9493	0.9125	0.9132
F1-Score	0.5587	0.6532	0.6144	0.6448

g) Generalizability evaluation

In this section, we evaluate the generalizability of our approach to publicly available datasets. It is important to discuss the steps involved for KW-DNN for the effective utilization of this approach on other datasets. The utilization of expert domain knowledge is crucial for the successful segmentation of any ROI from any imaging modality. This is achieved by processing the image for shapes, edges, or other patterns suggested by the expert, which leads to the acquisition of engineered features. To evaluate the generalizability of both datasets, hand-crafted features specific to phenotype and image modality are employed. For the dynamic infusion of knowledge, the engineered features are compared against the actual ground truth to determine the confidence level of each ROI. In the absence of ground truth for test images, the average confidence level is used to make decisions in a real scenario. The infusion of knowledge is performed on the optimal layer, and the weights are assigned dynamically based on the confidence level. The aforementioned procedure is employed to design a two-stage experiment. The objective of this experiment is to compare the performance of a knowledge-infused DNN with that of a conventional DNN on a publicly available medical segmentation dataset. Examples of images from each dataset can be observed in Fig. 10. In the first stage of the experiment, the kvasir polyp dataset [36] was chosen due to its value to researchers working on segmentation tasks. This dataset offers a diverse collection of images that can be used for training and evaluating segmentation models. Moreover, pixel-level segmentation masks can be employed to assess the accuracy of the models. The polyp RGB images without any pre-processing are used as input to the network. The external knowledge is infused at the optimal layer, which is extracted through blob detection. The detected blobs are then incorporated into the network. The performance of the conventional DNN is compared to the knowledge-infused DNN in Table 8. The infusion of external knowledge has shown to enhance pixel-level detection, which is evident by the increased value of IOU. The notable improvement in the F1-score provides evidence of the importance of external knowledge infusion in a deep learning network. The infusion of knowledge enforces domain knowledge in the internal layers of the network to prioritize important features. This leads to an improvement in the network's performance. In the second phase of our experiment, we utilized the publicly available DRIVE dataset [37] for vessel segmentation. This dataset comprises 40 images, with 20 images each for the test and train sets. A mask image is provided for every retinal image, indicating the region of interest. The original image is given as input to the network without any pre-processing. The knowledge is engineered by extracting the structuring elements from the image, which are then infused on the optimal layer based on the confidence level. The performance of the knowledge-infused network is compared with a deep learning network in Table 8. Our results indicate an improvement in both IOU and F1-score, demonstrating that the infusion of domain knowledge is equally applicable to small datasets. This improvement is due to the mechanism of the infused network to prioritize domain knowledge within the internal structure of the DNN. Our findings suggest that domain knowledge can effectively address the limitations of deep learning networks when working with small datasets.

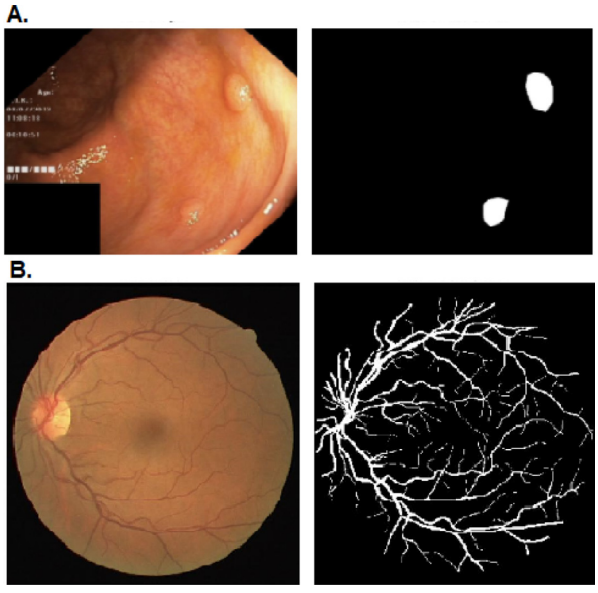

Fig. 10. A) Sample of Kvasir-SEG dataset [36]. B) Sample of DRIVE dataset [37].

5. Discussion

The primary goal of this paper is to enhance the effectiveness of deep learning methods in medical image analysis by integrating expert knowledge. Based on the neuro-symbolic AI approach, the Deepinfusion method proposed in this study incorporates the output of the knowledge model into the deep learning network layer as attention. By optimizing the weights of both models and dynamically selecting the infusion layer in the DNN, the adaptive infusion process significantly improves the detection and segmentation of ROI through the infusion of attention. To substantiate the effectiveness of the proposed method, we developed a neuro-symbolic AI method for DSA analysis, which combines the domain expert knowledge of identifying aneurysms from DSA images with data-driven deep learning techniques. The results indicate that the proposed approach enhances the detection and segmentation performance by incorporating expert knowledge, thereby overcoming the limitations of deep learning on small datasets, which is often the case in rare diseases, and the inability to share data in the cloud due to HIPPA compliance. The proposed Deepinfusion approach relies on the notion of measuring the confidence level of the hand-crafted machine learning/knowledge model on its prediction output and infusing the potential ROI as attention in the deep learning network layer, proportional to the certainty of those predictions. Since the DNN itself also processes the same DSA input, the induced attention of the knowledge model also assists the DNN in significantly improving ROI detection. The domain knowledge infusion-based deep learning model is expected to improve

the accuracy of various medical image analysis models when large-scale datasets are not available.

The expert-advised knowledge can be extracted using ML technique from the hand-crafted features. But these features may miss some important information. So, rather than using it as the input, the knowledge is introduced in the internal structure of the DNN. Due to the DNN's black-box nature, adaptive exploitation of the domain knowledge directly within the neural network is not possible. Therefore, we have created the equivalent feature map through the knowledge embeddings. The novelty of the proposed system is to dynamically infuse the domain knowledge directly into the DNN by selecting the appropriate layer of DNN and adjusting its weights proportion to the knowledge model. The infusion of external knowledge into deep neural networks is shown to enhance performance in the detection and segmentation of aneurysms, particularly when the dataset is challenging, such as those containing various atrial views, fluctuations in dye intensity, different sizes of regions of interest, and background noise. However, selecting the optimal infusion layer is complicated due to the complex architecture of deep learning models, which include ResNet blocks and skip connections. In this study, the impact of infused knowledge at the beginning, middle, and end of the deep neural network layer was investigated, with layers 57, 106, 209, 278, and 391 being selected for analysis. The introduction of knowledge at the end layer of the network improved the detection rate, but also produced significant noise due to lack of filtering through the deep layers. Infusion at layer 278 or 318 resulted in improved detection but low segmentation accuracy. Infusion of knowledge in the initial layer, specifically in layer 57, produced infused knowledge that behaves as an additional input and undergoes significant convolutions downstream. Segmentation was slightly improved over the model infused at the ending layers of the network but not as accurate in its contribution towards further analysis for rupture prediction. When infusion was performed near the middle of the encoder, as in layers 106 and 209, the model outperformed for aneurysm segmentation but may miss small aneurysms. The visualization of the last row shows that infusion improved segmentation accuracy and assisted the ability to detect an aneurysm when the arteries in DSA images were darker due to concentration of dye compared to the portion where aneurysm exists. Thus, adaptive infusion of knowledge is recommended to optimize performance in terms of segmentation and detection, with individual tailoring of infusion at different layers to improve system performance. The classified aneurysms can be categorized based on confidence levels, which can inform the decision of which infusion layer to use for each instance.

The concept of adaptive infusion involves infusing knowledge into dynamic layers of DNN with varying amounts of weight given to external knowledge and deep neural networks. The improvement in results on public datasets shows the importance of knowledge infusion (Fig. 11). The effectiveness of knowledge-infused networks on public datasets can be improved by adding domain experts, which helps to improve the knowledge engineering process. Domain experts provide insights for the extraction of knowledge. They can also help to identify potential problems and suggest solutions. Despite the high performance of the adaptive knowledge infusion, as the complexity and size of networks increase, more memory resources are required along with the learning time. Currently, the background information is also passed to the network along with the knowledge. In the future, the complexity may be reduced by infusing only the spatial aneurysm of the region of interest. Our long time goals include the implementation of a reinforcement learning-based knowledge-infused network to make adaptive real-time systems.

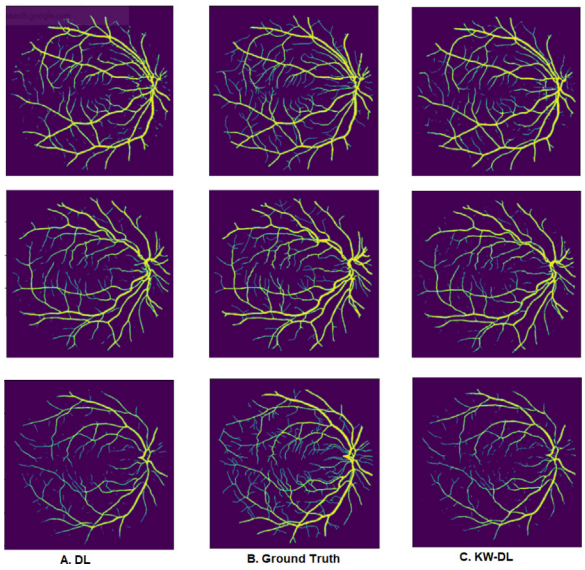

Fig. 11. Impact of knowledge infusion in segmentation of DRIVE images.

6. Conclusion

In medical image analysis, the focus of deep learning research to date has been on improving performance by optimizing model architectures and their parameters, and systematically altering/improving datasets. However, the power of infusing human intellect into the neural network remained largely unexplored. This paper has introduced a novel approach, adaptive knowledge exploitation on the traditional deep learning architecture, by implementing a DeepInfusion model for aneurysm detection and segmentation, which infuses medical expert knowledge into the deep learning layers. Empirical results highlight the importance of selecting the appropriate deep learning layer, along with the distribution of weights between the knowledge and deep features, to achieve optimal performance. In the future, we plan to extend the current system by optimizing the selection of the layer for knowledge infusion and more precise adjustments of the weight for infused knowledge in DNN to further improve the detection and segmentation.

CRediT authorship contribution statement

Iram Abdullah: Methodology, Software, Validation, Investigation, Writing - original draft, Writing - review & editing, Visualization. **Ali Javed:** Conceptualization, Methodology, Validation, Formal analysis, Investigation, Writing - original draft, Writing - review & editing, Supervision, Project administration. **Khalid Mahmood Malik:** Conceptualization, Methodology, Formal analysis, Investigation, Resources, Writing - original draft, Writing - review & editing, Supervision, Project administration, Funding acquisition. **Ghaus Malik:** Methodology, Resources, Data curation, Writing - review & editing.

Data availability

The authors do not have permission to share data.

Declaration of Competing Interest

The authors declare that they have no known competing financial interests or personal relationships that could have appeared to influence the work reported in this paper.

Acknowledgment

This work is supported by Brain Aneurysm Foundation USA. We also acknowledge the administrative and technical support of Henry Ford Health System, MI and Oakland University, MI.

References

[1] G. Boulouis, C. Rodriguez-Régent, E.C. Rasolonjatovo, W. Ben Hassen, D. Trystram, M. Edjlali-Goujon, J.-F. Meder, C. Oppenheim, O. Naggara, Unruptured intracranial aneurysms: An updated review of current concepts for risk factors, detection and management, Revue neurologique 173 (9) (2017) 542–551.
[2] Rafia Shahzad, Farhana Younas, Detection and characterization of intracranial aneurysms: magnetic resonance angiography versus digital subtraction angiography, J. Coll. Physicians Surg. Pak. 21 (6) (2011) 325–329.
[3] Syed Uzair Ahmed, J. Mocco, Xiangnan Zhang, Michael Kelly, Amish Doshi, Kambiz Nael, Reade De Leacy, Mra versus dsa for the follow-up imaging of intracranial aneurysms treated using endovascular techniques: a meta-analysis, J. Neurointerventional Surgery 11 (10) (2019) 1009–1014.
[4] Luke Tomycz, Neil K Bansal, Catherine R Hawley, Tracy L Goddard, Michael J Ayad, Robert A Mericle, real-world comparison of non-invasive imaging to conventional catheter angiography in the diagnosis of cerebral aneurysms, Surg. Neurol. Int. 2 (2011).
[5] Khalid Mahmood Malik, Shakeel M Anjum, Hamid Soltanian-Zadeh, Hafiz Malik, Ghaus M Malik, A framework for intracranial saccular aneurysm detection and quantification using morphological analysis of cerebral angiograms, IEEE Access 6 (2018) 7970–7986.
[6] Jian Zhang, Anil Can, Pui Man Rosalind Lai, Srinivasan Mukundan, Victor M Castro, Dmitriy Dligach, Sean Finan, Vivian S Gainer, Nancy A Shadick, Guergana Savova, et al., Morphological variables associated with ruptured basilar tip aneurysms, Sci. Rep. 11 (1) (2021) 1–9.
[7] Shaoxiong Ji, Shirui Pan, Erik Cambria, Pekka Marttinen, S. Yu Philip, A survey on knowledge graphs: Representation, acquisition, and applications, IEEE Trans. Neural Networks Learn. Syst. 33 (2) (2021) 494–514.
[8] Sungyong Seo, Sercan Arik, Jinsung Yoon, Xiang Zhang, Kihyuk Sohn, Tomas Pfister, Controlling neural networks with rule representations, Adv. Neural Inform. Process. Syst. 34 (2021) 11196–11207.
[9] Hidetaka Arimura, Qiang Li, Yukunori Korogi, Toshinori Hirai, Hiroyuki Abe, Yasuyuki Yamashita, Shigehiko Katsuragawa, Ryuji Ikeda, Kunio Doi, Development of cad scheme for automated detection of intracranial aneurysms in magnetic resonance angiography, Int. Congr. Ser., vol. 1268, Elsevier, 2004, pp. 1015–1020.
[10] Hidetaka Arimura, Qiang Li, Yukunori Korogi, Toshinori Hirai, Hiroyuki Abe, Yasuyuki Yamashita, Shigehiko Katsuragawa, Ryuji Ikeda, Kunio Doi, Automated computerized scheme for detection of unruptured intracranial aneurysms in three-dimensional magnetic resonance angiography1, Academ. Radiol. 11 (10) (2004) 1093–1104.
[11] Clemens M Hentschke, Oliver Beuing, Rosa Nickl, Klaus D Tönnies, Detection of cerebral aneurysms in mra, cta and 3d-ra data sets, Medical Imaging 2012: Computer-Aided Diagnosis, vol. 8315, International Society for Optics and Photonics, 2012, p. 83151I.
[12] Tim Jerman, Franjo Pernuš, Boštjan Likar, Žiga Špiclin, Blob enhancement and visualization for improved intracranial aneurysm detection, IEEE Trans. Visual Comput. Graphics 22 (6) (2015) 1705–1717.
[13] Stefan Bruckner, M. Eduard Gröller, Instant volume visualization using maximum intensity difference accumulation, Computer Graphics Forum, vol. 28, Wiley Online Library, 2009, pp. 775–782.
[14] Hira Khan, Muhammad Sharif, Nargis Bibi, Nazeer Muhammad, A novel algorithm for the detection of cerebral aneurysm using sub-band morphological operation, Eur. Phys. J. Plus 134 (1) (2019) 34.
[15] Yousra Zafar, Ali Javed, Khalid Mahmood Malik, Jeremy Santamaria, Ghaus Malik, A diagnostic system for intracranial saccular and fusiform aneurysms with location detection, in: 2021 IEEE EMBS International Conference on Biomedical and Health Informatics (BHI), IEEE, 2021, pp. 1–4.
[16] Shouhei Hanaoka, Yukihiro Nomura, Mitsutaka Nemoto, Soichiro Miki, Takeharu Yoshikawa, Naoto Hayashi, Kuni Ohtomo, Yoshitaka Masutani, Akinobu Shimizu, Hotpig: a novel geometrical feature for vessel morphometry and its application to cerebral aneurysm detection, in: International conference on medical image computing and computer-assisted intervention, Springer, 2015, pp. 103–110.
[17] Y. Uchiyama, H. Ando, R. Yokoyama, T. Hara, H. Fujita, T. Iwama, Computer-aided diagnosis scheme for detection of unruptured intracranial aneurysms in mr angiography, in: 2005 IEEE engineering in medicine and biology 27th annual conference, IEEE, 2006, pp. 3031–3034.
[18] Xiaojiang Yang, Daniel J Blezek, Lionel TE Cheng, William J Ryan, David F Kallmes, Bradley J Erickson, Computer-aided detection of intracranial aneurysms in mr angiography, J. Digital Imag. 24 (1) (2011) 86–95.
[19] Clemens M Hentschke, Oliver Beuing, Rosa Nickl, Klaus D Tönnies, Automatic cerebral aneurysm detection in multimodal angiographic images, in: 2011 IEEE Nuclear Science Symposium Conference Record, IEEE, 2011, pp. 3116–3120.
[20] Azadeh Firouzian, Rashindra Manniesing, Zwenneke H Flach, Roelof Risselada, Fop van Kooten, Miriam CJM Sturkenboom, Aa.d. van der Lugt, Wiro J Niessen, Intracranial aneurysm segmentation in 3d ct angiography: Method and quantitative validation with and without prior noise filtering, Eur. J. Radiol. 79 (2) (2011) 299–304.
[21] Tim Jerman, Franjo Pernus, Boštjan Likar, Žiga Špiclin, Aneurysm detection in 3d cerebral angiograms based on intra-vascular distance mapping and convolutional neural networks, in: 2017 IEEE 14th international symposium on biomedical imaging (ISBI 2017), IEEE, 2017, pp. 612–615.
[22] Takahiro Nakao, Shouhei Hanaoka, Yukihiro Nomura, Issei Sato, Mitsutaka Nemoto, Soichiro Miki, Eriko Maeda, Takeharu Yoshikawa, Naoto Hayashi, Osamu Abe, Deep neural network-based computer-assisted detection of cerebral aneurysms in mr angiography, J. Magn. Reson. Imaging 47 (4) (2018) 948–953.
[23] JunHua Liao, LunXin Liu, HaiHan Duan, YunZhi Huang, LiangXue Zhou, LiangYin Chen, ChaoHua Wang, et al., Using a convolutional neural network and convolutional long short-term memory to automatically detect aneurysms on 2d digital subtraction angiography images: Framework development and validation, JMIR Med. Inform. 10 (3) (2022).
[24] Yuwen Zeng, Xinke Liu, Nan Xiao, Youxiang Li, Yu.hua. Jiang, Junqiang Feng, Shuxiang Guo, Automatic diagnosis based on spatial information fusion feature for intracranial aneurysm, IEEE Trans. Med. Imaging 39 (5) (2019) 1448–1458.
[25] Hu. Tao, Heng Yang, Yu. Wei Ni, Zhuoyun Jiang Lei, Keke Shi, Yu. Jinhua, Gu. Yuxiang, Yuanyuan Wang, Automatic detection of intracranial aneurysms in 3d-dsa based on a bayesian optimized filter, BioMedical Eng. OnLine 19 (1) (2020) 1–18.
[26] Xinke Liu, Junqiang Feng, Wu. Zhenzhou, Zhonghao Neo, Chengcheng Zhu, Peifang Zhang, Yan Wang, Yu.hua. Jiang, Dimitrios Mitsouras, Youxiang Li, Deep neural network-based detection and segmentation of intracranial aneurysms on 3d rotational dsa, Intervent. Neuroradiol. 27 (5) (2021) 648–657.
[27] Hailan Jin, Yin Yin, Hu. Minghui, Guangming Yang, Lan Qin, Fully automated unruptured intracranial aneurysm detection and segmentation from digital subtraction angiography series using an end-to-end spatiotemporal deep neural network, Medical Imaging 2019: Image Processing, vol. 10949, SPIE, 2019, pp. 379–386.
[28] Paschalis Bizopoulos, Nicholas Vretos, and Petros Daras. Comprehensive comparison of deep learning models for lung and covid-19 lesion segmentation in ct scans. arXiv preprint arXiv:2009.06412, 2020.
[29] Xiao-Xia Yin, Le Sun, Fu. Yuhan, Lu. Ruiliang, Yanchun Zhang, U-net-based medical image segmentation, J. Healthcare Eng. (2022, 2022.).
[30] Hengshuang Zhao, Jianping Shi, Xiaojuan Qi, Xiaogang Wang, and Jiaya Jia. Pyramid scene parsing network. In Proceedings of the IEEE conference on computer vision and pattern recognition, pages 2881–2890, 2017.
[31] Abhishek Chaurasia, Eugenio Culurciello, Linknet: Exploiting encoder representations for efficient semantic segmentation, in: 2017 IEEE visual communications and image processing (VCIP), IEEE, 2017, pp. 1–4.
[32] Yu. Jun, Jing Li, Yu. Zhou, Qingming Huang, Multimodal transformer with multi-view visual representation for image captioning, IEEE Trans. Circuits Syst. Video Technol. 30 (12) (2019) 4467–4480.
[33] Jian Zhang, Yunyin Cao, Wu. Qun, Vector of locally and adaptively aggregated descriptors for image feature representation, Pattern Recogn. 116 (2021).
[34] Olaf Ronneberger, Philipp Fischer, Thomas Brox, U-net: Convolutional networks for biomedical image segmentation, in: International Conference on Medical image computing and computer-assisted intervention, Springer, 2015, pp. 234–241.
[35] Jiaxing Tan, Yumei Huo, Zhengrong Liang, Lihong Li, Expert knowledge-infused deep learning for automatic lung nodule detection, J. X-ray Sci. Technol. 27 (1) (2019) 17–35.
[36] Debesh Jha, Pia H Smedsrud, Michael A Riegler, Pål Halvorsen, Thomas de Lange, Dag Johansen, Håvard D Johansen, Kvasir-seg: A segmented polyp dataset, in: International Conference on Multimedia Modeling, Springer, 2020, pp. 451–462.
[37] Mingxing Li, Shenglong Zhou, Chang Chen, Yueyi Zhang, Dong Liu, Zhiwei Xiong, Retinal vessel segmentation with pixel-wise adaptive filters, in: 2022 IEEE 19th International Symposium on Biomedical Imaging (ISBI), IEEE, 2022, pp. 1–5.

Iram Abdullah is a Ph.D. scholar at the University of Engineering and Technology (UET), Taxila, Pakistan. Her research interests include the development of intelligent systems for medical diagnostics, with a focus on infusing knowledge in DNNs. She has 9 years of teaching experience and has been affiliated with HITEC University, Taxila, Punjab Tianjin University of Technology, and Bahria University Lahore campus campus.

Ali Javed (SM'16) received the B.Sc. degree with honors and 3rd position in Software Engineering from UET Taxila, Pakistan in 2007. He received his MS and Ph.D. degrees in Computer Engineering from UET Taxila, Pakistan in 2010 and 2016. He received Chancellor's Gold Medal in MS Computer Engineering degree. Dr. Javed is serving as an Associate Professor in Software Engineering Department at UET Taxila, Pakistan. He served as a Postdoctoral Scholar in the SMILES lab at Oakland University, MI, USA in 2019 and as a visiting Ph. D. scholar in the ISSF Lab at the University of Michigan, MI, USA in 2015. His areas of interest are Multimedia Forensics, Image Processing, Computer vision, Video Content Analysis, Medical Image Processing, and Multimedia Signal Processing. He has published more than 100 papers in leading journals and conferences including the IEEE Transactions. Dr. Javed is a recipient of various research grants from HEC Pakistan, the National ICT R n D Fund, NESCOM, and UET Taxila Pakistan. He has also served as a HOD in Software Engineering Department at UET Taxila in 2014. Dr. Javed got selected as an Ambassador of the Asian Council of Science Editors from Pakistan in 2016. He is also a member of the Pakistan Engineering Council since 2007.

Khalid Mahmood Malik received the Ph.D. degree from the Tokyo Institute of Technology in 2010. Currently he is an associate professor in the School of Engineering and Computer Science at Oakland University. Prior to that, he was with Sanyo Electric Co., Japan, and DTS Inc., Japan, as a Researcher and Project Manager of the Semantic Research Group, respectively. His research interests include the integrated area of multi-modal neuro symbolic federated learning, medical image analytics, automated knowledge graph construction, smart and connected vehicle security, and fake multimedia detection. He has published a total of eighty-five technical papers including fifty (50) journal publications and thirty-five (35) conference/workshop publications. Dr. Malik's research is supported by the multiple National Science Foundation awards, the Brain Aneurysm Foundation, and the Michigan Translational Research and Commercialization Innovation Hub, among others. He is a co-director of centers for cybersecurity and Pervasive Personalized Intelligence at Oakland University. He is a recipient of numerous accolades, not limited to Oakland's Young Investigator Research award (2018), SECS Outstanding Research award (2019) and Distinguished Associate Professor award (2021).

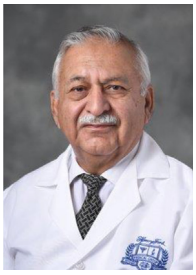

Ghaus M. Malik is currently the John R. Davis Chair and Executive Vice-Chair, Neurosurgery at Henry Ford Health System, Detroit, MI, USA. He specializes in cerebrovascular neurosurgery especially aneurysms and arteriovenous malformations. He has a 54 year of domain experience. His research interests include aneurysm rupture prediction, vasospasm, clinical outcomes of arteriovenous malformations (AVM), and genetic mechanisms for familial aneurysms and AVM.